A&A 381, 1026–1038 (2002)
DOI: 10.1051/0004-6361:20011596

Astronomy & Astrophysics

A survey of [HDCO]/[H_2CO] and [DCN]/[HCN] ratios towards low-mass protostellar cores

H. Roberts[1,⋆], G. A. Fuller[1], T. J. Millar[1], J. Hatchell[2], and J. V. Buckle[1,⋆⋆]

[1] Department of Physics, UMIST, PO Box 88, Manchester M60 1QD, UK
[2] Max-Planck-Institut für Radioastronomie, Auf dem Hügel 69, 53121 Bonn, Germany

Received 30 July 2001 / Accepted 5 October 2001

Abstract. We present observations of [HDCO]/[H_2CO] and [DCN]/[HCN] ratios towards a selection of low-mass protostellar cores in three different star forming regions. The best fit to the observed [HDCO]/[H_2CO] ratios is ∼0.05–0.07, similar to the values observed towards the dark clouds, TMC-1 and L134N. [DCN]/[HCN] ratios are ∼0.04, higher than those seen in TMC-1, around the low-mass protostar IRAS 16293 and the Orion Hot Core, but similar values to the Orion Compact Ridge and L134N. We compare our results with predictions from detailed, chemical models, and to other observations made in these sources. We find best agreement between models and observations by assuming that interaction between gas phase molecules and dust grains has impacted on the chemistry during the cold pre-collapse phase of the cloud's history. The abundance of deuterated species indicates that the dense gas out of which a low mass protostar forms, evolves and collapses on a timescale of ≤50 000 years. We find no marked difference between molecular D/H ratios towards different regions, or between Class 0 and Class I protostars. However, the striking difference between the [DCN]/[HCN] ratios we have measured and those previously observed towards Hot Molecular Cores leads us to suggest that there are significant evolutionary differences between high and low mass star forming regions.

Key words. ISM: molecules – ISM: clouds – ISM: abundances – stars: formation

1. Introduction

Observations of deuterated molecules have become an important tool in the study of interstellar chemistry. Although the underlying (or cosmic) D/H ratio is low ($\sim 10^{-5}$), the formation of deuterated molecules is preferred at low temperatures (≤80 K) and leads to a high degree of fractionation in cold, dark clouds. For example, in the quiescent dark cloud, TMC-1, molecular D/H ratios, including [HDCO]/[H_2CO] and [DCN]/[HCN] are observed to be $>10^{-2}$.

Enhanced molecular D/H ratios are also observed in hot molecular cores (HMC's), clumps of hot, dense gas, usually associated with high mass star formation. The temperatures of these cores (typically 70–150 K) should be high enough to preclude the enhancement of molecular D/H ratios through gas-phase reactions. However, the ratios which have been measured are generally $\sim 10^{-3}$ (e.g. Hatchell et al. 1998, 1999), lower than TMC-1, yet still enhanced over the cosmic value. It is now generally accepted that these ratios have been preserved from an earlier, colder phase of the cloud's history in the ice-mantles of dust grains. Once some heating event, such as the formation of a star or the passage of a shock, heats the grains sufficiently to evaporate their mantles, the D/H ratios can survive for $\sim 10^4$ yrs in the hot gas (Rodgers & Millar 1996).

In cold cores which are forming low mass stars, we might expect a situation intermediate between hot cores and dark clouds. To date, the only survey of deuterated molecules in a low-mass star forming region has been that of IRAS 16293–2422 (hereafter, IRAS 16293), a class 0, proto-binary system in ρ Oph, by van Dishoeck et al. (1995). However, their survey revealed discrepancies in the levels of fractionation of different molecules, with over 10% deuteration seen in species such as HDCO and HDS, yet only a few percent in species such as DCN. While the [DCN]/[HCN] ratio is similar to that observed in TMC-1, the [HDCO]/[H_2CO] ratio is at least twice as high. Neither the very large [HDCO]/[H_2CO] or [HDS]/[H_2S] ratios can be explained by a standard gas-phase chemistry.

We wished to confirm whether these high D/H ratios were a general feature of low-mass star formation, or particular to IRAS 16293. Therefore we have carried

Send offprint requests to: H. Roberts,
e-mail: hroberts@mps.ohio-state.edu
⋆ *Present address:* Ohio State University, Columbus, Ohio.
⋆⋆ *Present address:* Joint Astronomy Centre, Hilo, Hawaii.

Table 1. Sources observed, along with velocities, bolometric temperatures and protostellar class taken from the literature.

Region	Source	α_{1950} [h m s]	δ_{1950} [° ′ ″]	$v_{\rm lsr}$ (km s^{-1})	$T_{\rm bol}$ (K)	Class
Perseus	B5 IRS1	03:44:31.7	+32:42:29	10.2	85	I
	L1448 mms	03:22:34.3	+30:33:35	5.6	56	0
	L1448 NW	03:22:31.1	+30:35:3.8	5.0	24	0
	HH211	03:40:48.7	+31:51:24	9.2	30	0
	IRAS 03282	03:28:15.2	+30:35:14	7.0	26	0
Taurus	L1527	04:36:49.3	+25:57:16	5.6	59	0
	L1551 IRS5	04:28:40.2	+18:01:42	6.4	97	I
Orion	RNO43	05:29:30.6	+12:47:25	9.6	33	0
	HH111	05:49:9.3	+02:47:48	8.5	38	0

Table 2. Molecular line list.

Transition	$\nu_{\rm ul}$ (GHz)	$E_{\rm u}$ (cm^{-1})	$A_{\rm ul}$ (s^{-1})
H_2CO $2_{1,1}$–$1_{1,0}$ (ortho)	150.498	15.7	6.468×10^{-5}
H_2CO $5_{1,4}$–$5_{1,5}$ (ortho)	72.409	45.8	8.011×10^{-7}
$H_2^{13}CO$ $2_{1,2}$–$1_{1,1}$ (ortho)	137.450	15.1	4.928×10^{-5}
HDCO $2_{1,1}$–$1_{1,0}$	134.285	9.3	4.587×10^{-5}
HDCO $4_{0,4}$–$3_{0,3}$[a]	256.585	21.5	4.736×10^{-4}
HCN 1-0 (triplet)	88.632	2.96	2.426×10^{-5}
$H^{13}CN$ 1-0 (triplet)	86.340	2.88	2.224×10^{-5}
$HC^{15}N$ 1-0	86.055	2.87	2.203×10^{-5}
DCN 1-0 (triplet)	72.415	2.42	1.312×10^{-5}
DCN 2-1 (multiplet)[b]	144.828	7.25	1.259×10^{-4}
c-C_3HD $2_{2,0}$–$1_{1,1}$[c]	137.455	6.27	5.335×10^{-5}

[a] Observed towards only three sources, due to high $T_{\rm SYS}$.
[b] Observed by Buckle & Fuller (2001).
[c] Tentative identification of lines seen in the $H_2^{13}CO$ band.

out a survey to measure both the [HDCO]/[H_2CO] and [DCN]/[HCN] ratios in the dense gas associated with young protostars ('protostellar cores') in three different star forming regions. Our sources are listed in Table 1.

Sections 2 and 3 describe the observations and data reduction techniques, presenting the resulting column densities and molecular D/H ratios, Sect. 4 summarises and discusses these results. In Sect. 5 we describe the chemical models and compare model predictions with the observations. Section 6 compares these results with those from previous observations of high-mass star forming regions.

Throughout, we adopt the conventions; "N(ABC)" for the column density of molecule ABC, "[ABC]" for N(ABC)/N(H_2), i.e. the fractional abundance of molecule ABC, and "fractionation of XD" for [XD]/[XH].

2. Observations

The observations were carried out using the NRAO 12 m radio telescope, at Kitt Peak, Arizona, in November 1999, Table 2 lists the observed transitions.

The 3 mm receivers were used to observe the HCN 1–0 and DCN 1–0 transitions, the H_2CO $5_{1,4}$–$5_{1,5}$ transition frequency being covered by the DCN 1–0 band, the 2 mm receivers were used for the H_2CO $2_{1,1}$–$1_{1,0}$, HDCO $2_{1,1}$–$1_{1,0}$ and $H_2^{13}CO$ $2_{1,2}$–$1_{1,1}$ transitions and the 1 mm receivers were used for the HDCO $4_{0,4}$–$3_{0,3}$ line. The MAC spectrometer was in 2 IF mode with 16 384 channels. The $H^{13}CN$ and $HC^{15}N$ transitions were observed simultaneously, with the 3 mm receiver, using 4 IF mode with an offset of 285 MHz between the pairs of filter banks, though in the end, the $HC^{15}N$ lines were not above the level of the noise. In all cases the spectra were observed using 24 kHz channels, giving a velocity resolution of ∼0.04 km s^{-1}, except for the DCN 2–1 spectra, observations of which are described in Buckle & Fuller (2001).

The weather was clear, with typical sytem temperatures of 180–300 K for the 3 mm receiver and 200–350 K for the 2 mm receiver, while for the brief time we used the 1 mm receiver, the system temperature rose to ∼1000 K. Pointing was checked every two hours or so and errors found to be ∼5–6″.

All data were calibrated by the usual chopper wheel method and corrected for $\eta_{\rm m}^*$, the efficiency at which the source couples to the main diffraction beam, to give $T_{\rm MB}$. In all cases we have assumed a filling factor of 1, i.e. we have assumed that the source fills the main diffraction beam of the telescope. This may not be strictly true for our low-frequency transitions (the beamwidth of the 12 m telescope is 90″ at 70 GHz), however, as we are primarily interested in the ratios of our column densities, any errors introduced by this assumption should cancel out.

The spectra we obtained are shown in Figs. 1 and 2. In general, we saw less molecular line emission towards the Orion sources, though the $H^{13}CN$ spectra towards RNO43 and HH111 are particularly noisy. HCN 1–0 lines towards L1448 mms, L1448 NW and L1551 IRS5 show significant self-absorption, particularly in the main component of the triplet. The additional lines seen in the $H_2^{13}CO$ band towards B5 IRS1, L1448 mms, L1448 NW and L1527 have been tentatively identified as the $2_{2,0}$–$1_{1,1}$ transition of deuterated cyclopropenylidene (c-C_3HD) at 137.455 GHz. The H_2CO $5_{1,4}$–$5_{1,5}$ transition was not seen towards any of the sources. Spectra of the DCN 2–1 transition have been presented in Buckle (2001).

Tables 3 and 4 present linewidths and integrated intensities from Gaussian fits to the lines, or 3σ upper limits on the non-detections. For the HCN 1–0 triplet transition, which is likely to have significant optical depth, we made

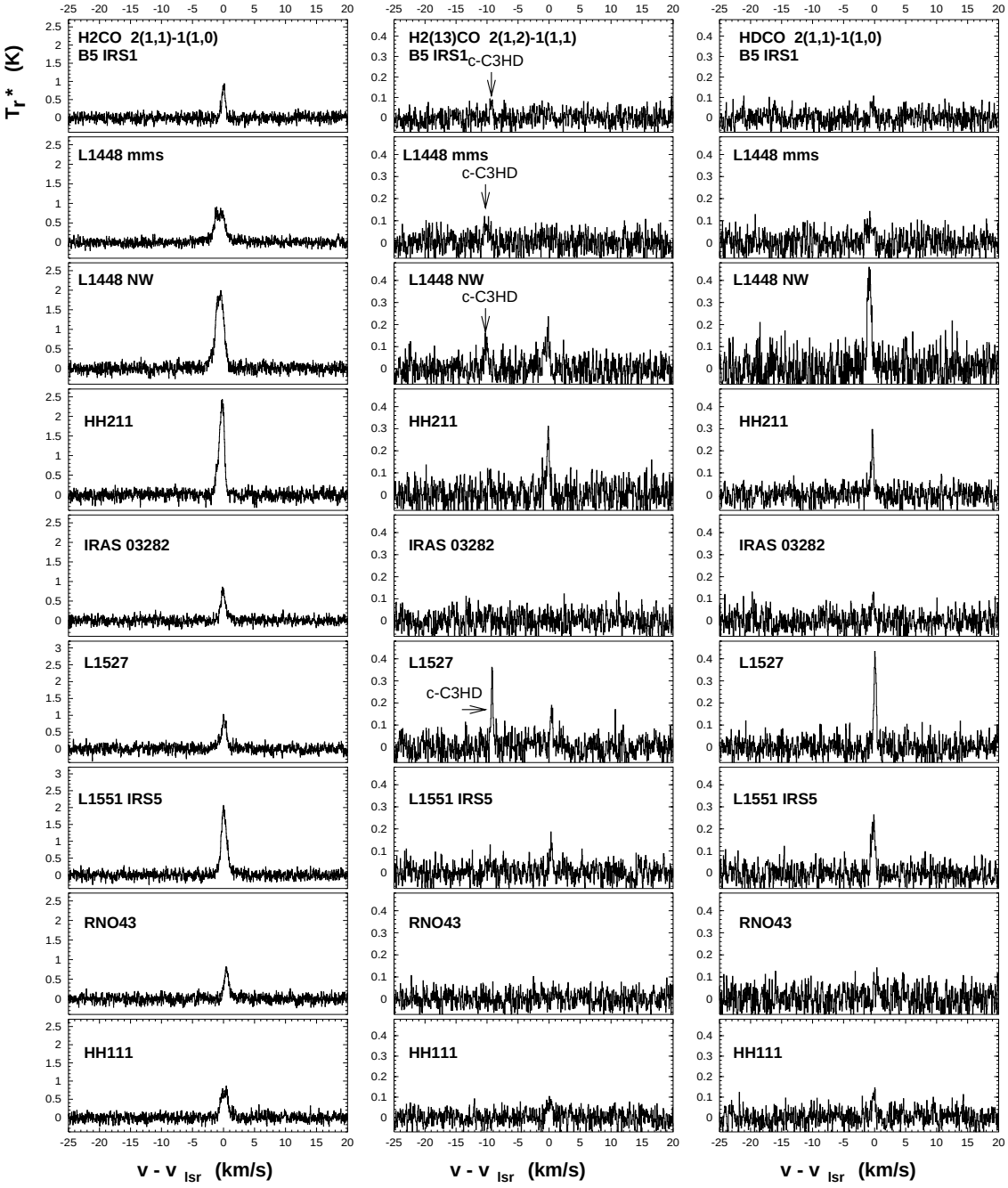

Fig. 1. Spectra of H_2CO (left), $H_2^{13}CO$ (centre) and HDCO (right) observed towards the sources in our survey. The $3_{1,2}$–$2_{2,1}$ transition of c-C_3HD has been tentatively identified in the $H_2^{13}CO$ spectra towards B5 IRS1, L1448 mms, L1448 NW and L1527.

use of the "HFS" method of the data reduction software package "CLASS", which attempts to fit the three lines in an LTE approximation, and returns an estimate for the average linewidth and for the optical depth of the main component. For the other multiplet transitions we measured the integrated intensity of the strongest component of the multiplet, then corrected the column densities for the expected statistical weight of the strongest line at LTE; 0.556 for $H^{13}CN$ and DCN 1–0, and 0.446 for DCN 2–1.

Uncertainties in $\int T_{\rm MB} {\rm d}v$ were estimated from the noise in the spectra. For the HCN 1–0, DCN 1–0 and H_2CO $2_{1,1}$–$1_{1,0}$ transitions the lines were strong compared to the noise and the uncertainties in $\int T_{\rm MB} {\rm d}v$ are better than 15%. For the HDCO $2_{1,1}$–$1_{1,0}$, $H_2^{13}CO$ $2_{1,2}$–$1_{1,1}$, $H^{13}CN$ 1–0 and DCN 2–1 transitions the uncertainties are mostly between 15 and 30%, though a few scans have uncertainties of >40%.

3. Data reduction

3.1. Formaldehyde

The formulae which connect the integrated intensity of a rotational transition with the number of emitting

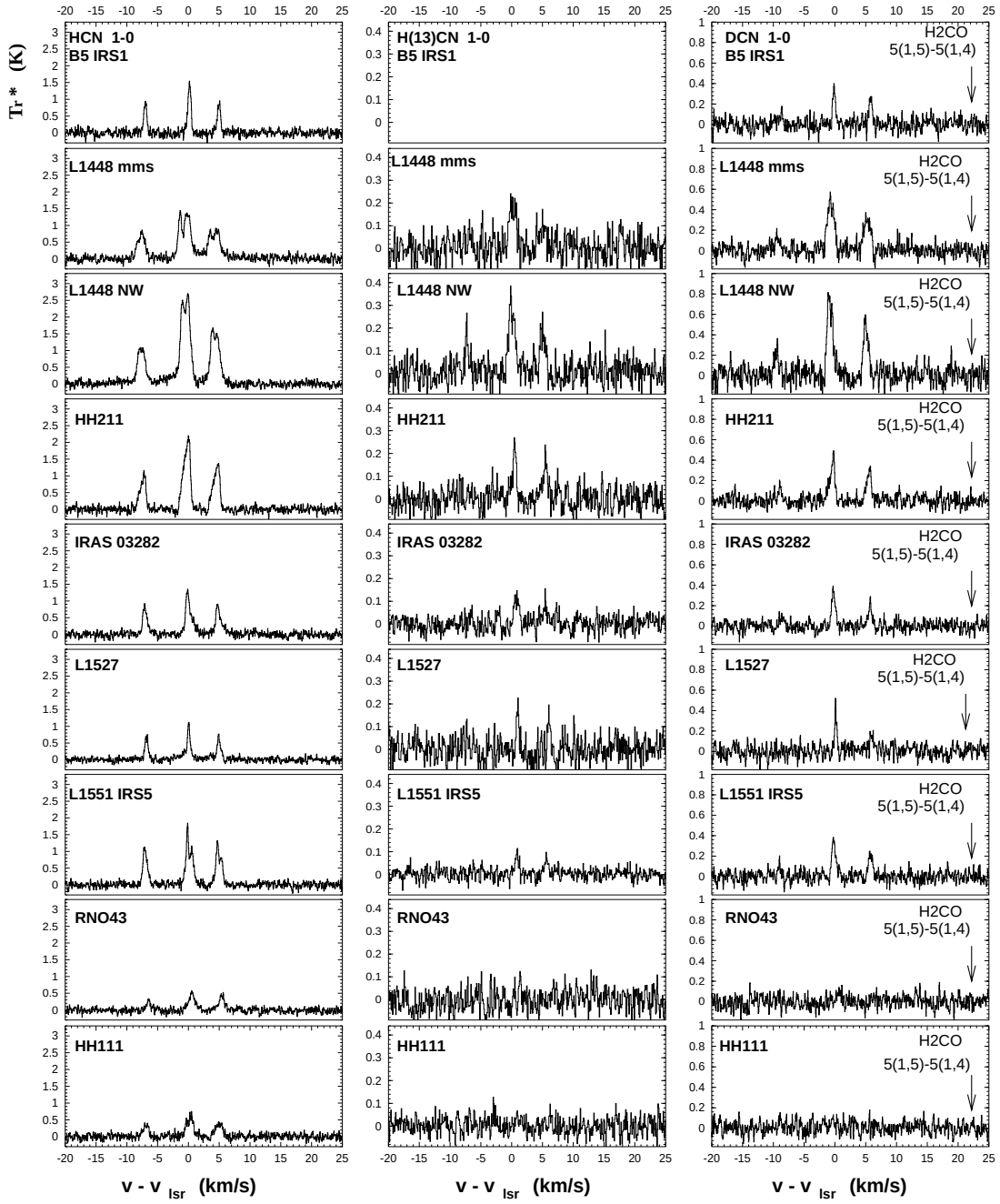

Fig. 2. Spectra of HCN (left), $H^{13}CN$ (centre) and DCN (right) obtained towards the sources in our survey. The approximate expected position of the H_2CO $5_{1,4}$–$5_{1,5}$ transition is indicated on each DCN spectra.

molecules are, for an optically thin transition, neglecting background radiation[1];

$$\int T_{\rm MB}\,{\rm d}v = \frac{A_{\rm ul}hc^3}{8\pi k\nu^2}\,N_{\rm u} \tag{1}$$

and, assuming the system is in LTE;

$$N_{\rm u} = \frac{g_{\rm u}}{Q(T_{\rm ex})}{\rm e}^{-E_{\rm u}/kT_{\rm ex}}N_{\rm TOT} \tag{2}$$

[1] For low-excitation lines this may not be entirely correct, but we estimate that the additional error introduced will be no more than 20% for $T_{\rm ex} \sim 10$ K.

(see, for example, Goldsmith & Langer 1999). Where $N_{\rm u}$ is the column density of molecules in the upper level of the transition, $N_{\rm TOT}$ is the total column density of emitting molecules and $Q(T_{\rm ex})$ is the partition function.

For a line which has significant optical depth, a correction factor can be applied to the above formulae;

$$G(\tau) = \int \frac{1-\exp(-\tau\phi(v))}{\tau\Delta(v)}{\rm d}v \tag{3}$$

(Stutzki et al. 1989), an integral which has been approximated as;

$$G(\tau) \sim \frac{1-\exp(-\tau')}{\tau'} \tag{4}$$

Table 3. Linewidths and integrated intensities for the observed transitions of formaldehyde and deuterated cyclopropenylidene, 1σ uncertainties are given in brackets, upper limits are 3σ.

Line	Source	Δv ($\mathrm{kms^{-1}}$)	$\int T_{\rm MB}\mathrm{d}v$ (K $\mathrm{km\,s^{-1}}$)
H_2CO	B5 IRS1	0.66 (±0.02)	0.771 (±0.077)
$2_{1,1}$–$1_{1,0}$	L1448 mms	1.96 (±0.03)	2.013 (±0.181)
	L1448NW	1.53 (±0.02)	3.962 (±0.198)
	HH211	1.02 (±0.01)	3.152 (±0.126)
	IRAS 03282	0.96 (±0.03)	0.934 (±0.100)
	L1527	1.02 (±0.04)	1.120 (±0.123)
	L1551 IRS5	1.08 (±0.01)	2.722 (±0.136)
	RNO43	0.88 (±0.03)	0.873 (±0.096)
	HH111	1.33 (±0.03)	1.342 (±0.161)
H_2CO	B5 IRS1	—	<0.069
$5_{1,4}$–$5_{1,5}$	L1448 mms	—	<0.171
	L1448 NW	—	<0.249
	HH211	—	<0.078
	IRAS 03282	—	<0.141
	L1527	—	<0.069
	L1551 IRS5	—	<0.105
	RNO43	—	<0.156
	HH111	—	<0.201
$H_2^{13}CO$	B5 IRS1	—	<0.074
$2_{1,2}$–$1_{1,1}$	L1448 mms	—	<0.090
	L1448NW	0.99 (±0.09)	0.164 (±0.061)
	HH 211	0.48 (±0.06)	0.166 (±0.071)
	IRAS 03282	—	0.090
	L1527	0.44 (±0.05)	0.100 (±0.027)
	L1551 IRS5	0.52 (±0.07)	0.080 (±0.016)
	RNO43	—	<0.078
	HH 111	0.97 (±0.13)	0.095 (±0.047)
HDCO	B5 IRS1	0.67 (±0.10)	0.054 (±0.034)
$2_{1,1}$–$1_{1,0}$	L1448 mms	1.28 (±0.14)	0.126 (±0.077)
	L1448 NW	0.72 (±0.04)	0.405 (±0.069)
	HH211	0.44 (±0.03)	0.149 (±0.021)
	IRAS 03282	0.52 (±0.10)	0.073 (±0.030)
	L1527	0.44 (±0.02)	0.237 (±0.026)
	L1551 IRS5	0.71 (±0.04)	0.210 (±0.036)
	RNO43	—	<0.108
	HH111	0.60 (±0.08)	0.110 (±0.051)
c-C_3HD	B5 IRS1	0.46 (±0.06)	0.049 (±0.021)
$2_{2,0}$–$1_{1,1}$	L1448 mms	1.00 (±0.12)	0.100 (±0.040)
	L1448 NW	0.75 (±0.10)	0.106 (±0.046)
	L1527	0.35 (±0.03)	0.153 (±0.021)

Table 4. For HCN 1–0; the average linewidth and total integrated intensity of the triplet state. For $H^{13}CN$ and DCN; linewidths and integrated intensities for the strongest component of each multiplet transition. 1σ uncertainties are given in brackets, upper limits are 3σ.

Line	Source	Δv ($\mathrm{kms^{-1}}$)	$\int T_{\rm MB}\mathrm{d}v$ (K $\mathrm{km\,s^{-1}}$)
HCN	B5 IRS1	0.43 (±0.01)	0.542 (±0.705)
1–0	L1448 mms	1.48 (±0.03)	1.747 (±0.140)
	L1448 NW	1.40 (±0.01)	4.576 (±0.275)
	HH211	1.01 (±0.01)	2.127 (±0.149)
	IRAS 03282	0.69 (±0.02)	0.688 (±0.083)
	L1527	0.48 (±0.02)	0.391 (±0.070)
	L1551 IRS5	0.74 (±0.01)	0.877 (±0.096)
	RNO43	0.99 (±0.05)	0.584 (±0.123)
	HH111	0.89 (±0.05)	0.949 (±0.247)
$H^{13}CN$	B5 IRS1[a]	—	—
1–0	L1448 mms	1.11 (±0.07)	0.299 (±0.057)
	L1448 NW	1.27 (±0.08)	0.460 (±0.069)
	HH211	0.83 (±0.10)	0.206 (±0.037)
	IRAS 03282	0.91 (±0.07)	0.129 (±0.036)
	L1527	0.41 (±0.06)	0.092 (±0.022)
	L1551 IRS5	0.62 (±0.07)	0.114 (±0.024)
	RNO43	—	<0.135
	HH111	—	<0.117
DCN	B5 IRS1	0.49 (±0.04)	0.200 (±0.030)
1–0	L1448 mms	1.27 (±0.06)	0.681 (±0.075)
	L1448 NW	1.01 (±0.05)	0.843 (±0.084)
	HH211	0.92 (±0.07)	0.397 (±0.052)
	IRAS 03282	0.71 (±0.04)	0.267 (±0.032)
	L1527	0.39 (±0.03)	0.180 (±0.023)
	L1551 IRS5	0.73 (±0.05)	0.285 (±0.037)
	RNO43	—	<0.144
	HH111	—	<0.141
DCN	B5 IRS1	0.57 (±0.05)	0.131 (±0.042)
2–1	L1448 mms	1.07 (±0.09)	0.476 (±0.071)
	L1448 NW	1.03 (±0.09)	0.515 (±0.041)
	HH211	0.81 (±0.06)	0.224 (±0.029)
	IRAS 03282	0.64 (±0.05)	0.180 (±0.034)
	L1527	—	<0.111
	L1551 IRS5	0.85 (±0.07)	0.233 (±0.037)
	RNO43	0.81 (±0.08)	0.121 (±0.034)
	HH111	—	<0.153

[a] Source not observed at this frequency.

where $\tau' = 0.679\,\tau^{0.911}$, by Wyrowski et al. (1999) for a Gaussian line profile, with an error of 4% for $0.01 < \tau < 10$ (15% for $0.01 < \tau < 100$).

As formaldehyde is abundant in molecular clouds, the $H_2CO\,2_{1,1}$–$1_{1,0}$ transition is likely to have significant optical depth. In order to estimate this we have used the ratios of $\int T_{\rm MB}\mathrm{d}v$ for the transitions of the main isotopomer and of the ^{13}C substitute.

Combining Eqs. (1) and (2), applying the correction factor, Eq. (4), for the H_2CO transition only, assuming a $^{12}C/^{13}C$ abundance ratio 60, and equal excitation and filling factors for the lines, then we expect that;

$$\frac{\int T_{\rm MB}\,\mathrm{d}v_{12}}{\int T_{\rm MB}\,\mathrm{d}v_{13}} = 60\,\frac{\nu_{13}^2}{\nu_{12}^2}\,\frac{A_{\rm ul(12)}}{A_{\rm ul(13)}}\left(\frac{1-\exp(-\tau')}{\tau'}\right) \sim 65.7\,\left(\frac{1-\exp(-\tau')}{\tau'}\right) \quad (5)$$

where a subscript "12" implies H_2CO, "13" implies $H_2^{13}CO$. Optical depths for the $H_2CO\,2_{1,1}$–$1_{1,0}$ transition can then be calculated.

The optical depths for the H_2CO transitions, listed in Table 5, are all less than 12, therefore, as we expect the isotope-substituted species to be between 10 and 100 times

Table 5. Optical depths for the H_2CO $2_{1,1}$–$1_{1,0}$ and HCN 1–0 transitions, along with excitation temperatures calculated for HCN and DCN and upper limits on T_{ex} for H_2CO.

Source	Optical Depth		Excitation temp. (K)		
	τ_{H_2CO}	τ_{HCN}	H_2CO	HCN	DCN
B5 IRS1	<11.5	10.7	<20	5	5
L1448 mms	<4.6	8.6	<31	5	5
L1448 NW	4.2	8.9	<27	8	5
HH211	5.8	9.0	<15	6	4
IRAS 03282	<11.5	9.0	<27	5	5
L1527	10.8	7.5	<18	4	<5
L1551 IRS5	2.4	16.9	<24	5	6
RNO43	<11.5	2.2	<30	4	>6
HH111	8.2	3.9	<33	5	—

less abundant than the main species, it seems reasonable to assume that our $H_2^{13}CO$ and HDCO transitions will be optically thin. We, thus, use Eqs. (1) and (2), connecting $\int T_{MB}\,dv$ and upper-level column density, N_u. We have also calculated the H_2CO column densities using these equations, but applying the correction factor in Eq. (4).

Limits on the excitation temperatures of H_2CO can be calculated, using the upper limits on the integrated intensity of the H_2CO $5_{1,4}$–$5_{1,5}$ transition, via

$$\frac{N_i}{N_j} = \frac{g_i}{g_j}\ \exp\left(\frac{E_j - E_i}{kT_{ex}}\right) \tag{6}$$

and are listed in Table 5. In calculating total column densities for H_2CO, $H_2^{13}CO$ and HDCO we have, therefore, used a range of excitation temperatures between 5 and 40 K, though, in fact, for $T_{ex} \geq 10$ K the column densities are not very sensitive to the assumed excitation temperature.

H_2CO and $H_2^{13}CO$ can exist in both ortho and para forms, depending on the alignment of the spins on the two hydrogens. In this study we have only observed transitions of ortho-H_2CO, therefore we need to correct our column densities for these molecules by some assumed ortho/para ratio. The high-temperature statistical value for this ratio is 3:1, however the actual ratio can depend on the temperatures at which the molecules formed, and so may be lower in cold clouds. Kahane et al. (1984), attempted to measure the H_2CO ortho:para ratio towards TMC-1. They obtained a best fit to their data of 1:1, but with large associated errors meaning that their observations could also be fit by a higher ratio.

The ortho/para ratio can be used to provide information on the formation mechanisms of molecules. Minh et al. (1995), who observed $H_2^{13}CO$ in the quiescent cores TMC-1 and L134N, found an ortho/para ratio very close to the statistical value of 3. This suggests that these molecules formed in the gas-phase. Dickens & Irvine (1999) observed H_2CO towards star-forming cores, finding the ortho/para ratio to be between 1.5 and 2, indicating that it has been modified due to formation and/or equilibration of H_2CO on grains.

We have currently adopted the statistical ratio of 3:1, However we note that adopting a ratio of 1:1 would increase our H_2CO column densities by a factor of 3/2, and so reduce the D/H ratios by 2/3, while assuming a ratio of of 2:1, as seen towards other star-forming cores, would only increase the H_2CO column densities by a factor of 9/8.

Table 6. Column densities for H_2CO, $H_2^{13}CO$ and HDCO, calculated over a range of excitation temperatures.

Source	5 K	10 K	20 K	30 K	40 K
	$N(H_2CO)$ ($\times 10^{13}$ cm^{-2})				
B5 IRS1	8.64	1.94	0.78	2.58	3.24
L1448 mms	12.2	2.73	2.79	3.62	4.55
L1448 NW	33.3	7.48	7.65	9.92	12.5
HH211	33.8	7.60	7.77	10.1	12.7
IRAS 03282	10.5	2.35	2.41	3.13	3.92
L1527	20.5	4.60	4.71	6.11	7.68
L1551 IRS5	16.2	3.64	3.73	4.83	6.07
RNO43	9.79	2.20	2.25	2.92	3.67
HH111	19.3	4.32	4.42	5.74	7.21
	$N(H_2^{13}CO)$ ($\times 10^{12}$ cm^{-2})				
B5 IRS1	<2.14	<5.24	<5.61	<7.39	<9.35
L1448 mms	<2.60	<0.64	<0.68	<0.90	<1.14
L1448 NW	4.73	1.16	1.24	1.64	2.07
HH211	4.79	1.18	1.26	1.66	2.10
IRAS 03282	<2.60	<0.64	<0.68	<0.90	<1.14
L1527	2.89	0.71	0.76	1.00	1.26
L1551 IRS5	2.31	0.57	0.61	0.80	1.01
RNO43	<2.25	<0.55	<0.59	<0.78	<0.99
HH111	2.74	0.67	0.72	0.95	1.20
	N(HDCO) ($\times 10^{12}$ cm^{-2})				
B5 IRS1	1.68	0.61	0.69	0.96	0.13
L1448 mms	3.93	1.41	1.62	2.23	2.91
L1448 NW	12.6	4.54	5.19	7.18	9.35
HH211	4.65	1.67	1.91	2.64	3.44
IRAS 03282	2.28	0.82	0.94	1.29	1.68
L1527	8.52	3.06	3.50	4.84	6.30
L1551 IRS5	6.55	2.35	2.69	3.72	4.85
RNO43	<3.37	<1.21	<1.39	<1.91	<2.49
HH111	3.43	1.23	1.41	1.95	2.54

The resulting column densities are given in Table 6. In Table 7 we give [HDCO]/[H_2CO] ratios at $T_{ex} = 10$ K, which is consistent with the limits on $T_{ex}(H_2CO)$ in all sources. As the molecular D/H ratios are not very sensitive to temperature, the uncertainty in T_{ex} is swamped by the uncertainty arising from the noise in the spectra. The large uncertainties on the [HDCO]/[H_2CO] ratios towards B5 IRS1, L1448 mms and IRAS 03282 are due to the fact that we only have an upper limit on the optical depth of the H_2CO 2–1 transition towards these sources.

3.2. Hydrogen cyanide

For the HCN 1–0 transition we obtained τ from the "HFS" method of CLASS. We then calculated the radiation

Table 7. [HDCO]/[H_2CO] for $T_{ex} = 10$ K.

Source	$\frac{N(HDCO)}{N(H_2^{13}CO)\times 60}$	$\frac{N(HDCO)}{N(H_2CO)}$
B5 IRS1	>0.019	0.066 (±0.050)
L1448 mms	>0.037	0.069 (±0.027)
L1448 NW	0.065 (±0.026)	0.061 (±0.013)
HH211	0.024 (±0.011)	0.022 (±0.004)
IRAS 03282	>0.021	0.073 (±0.050)
L1527	0.072 (±0.021)	0.066 (±0.013)
L1551 IRS5	0.069 (±0.017)	0.065 (±0.013)
RNO43	—	<0.117
HH111	0.031 (±0.021)	0.029 (±0.014)

temperature, ΔT_R, of each triplet by correcting T_{MB} for the main beam efficiency, η_{mb}, (∼0.61 at 88.6 GHz) and estimated excitation temperatures, T_{ex}, from the equation;

$$\Delta T_R = [J_\nu(T_{ex}) - J_\nu(T_{bg})]\left(1 - e^{-\tau}\right) \quad (7)$$

where T_{bg} is the temperature of the cosmic background radiation, 2.7 K. Optical depths and excitation temperatures for HCN are listed in Table 5.

Column densities for HCN were calculated using;

$$N = \frac{8\pi\nu_{ul}^3}{c^3}\frac{Q(T_{ex})}{g_u A_{ul}}\Delta v \frac{e^{E_u/kT_{ex}}}{e^{h\nu/kT_{ex}} - 1}\tau_{ul} \quad (8)$$

(Tiné et al. 2000), where ν_{ul} is the frequency of the unsplit transition, $Q(T_{ex})$ is the rotational partition function and Δv is the average *FWHM* linewidth, all other symbols have their usual meanings[2].

We calculated column densities for $H^{13}CN$ and DCN assuming optically thin lines (Eqs. (1) and (2)). As we observed two transitions of DCN, excitation temperatures could be calculated via Eq. (6). Values for T_{ex}(DCN) are listed in Table 5.

We note that effects such as beam dilution and/or self reversal in the HCN lines, may lead us to underestimate excitation temperatures for HCN. However, these temperatures are in good agreement, within the uncertainties arising from the spectral noise, with the excitation temperatures of DCN.

Column densities for HCN, $H^{13}CN$ and DCN, along with [DCN]/[HCN] ratios, are given in Table 8. In calculating $N(H^{13}CN)$ we have assumed excitation temperatures equivalent to T_{ex}(DCN).

L1448 NW and L1551 IRS5 are the only sources in which [DCN]/[HCN] ratios calculated from observations of HCN do not agree well with those calculated using $N(H^{13}CN)$. This is most likely due to errors in our estimation of the integrated intensity and/or optical depth of the HCN 1–0 transitions due to self absorption, and so we prefer the values derived from $N(H^{13}CN)$.

[2] As $\int T_R dv$ has been approximated by $T_R \Delta v$ in this formula, a factor of ∼1.06, which relates the integrated intensity of a Gaussian profile to the *FWHM*, has been neglected.

3.3. Cyclopropenylidene

The $3_{1,2}$–$2_{2,1}$ transition of c-C_3H_2 has previously been observed towards most of the sources in our survey (Buckle & Fuller 2001) and minimum column densities calculated. We have tentative detections of the $2_{2,0}$–$1_{1,1}$ transition of the deuterated counterpart of this molecule, c-C_3HD, towards 4 sources, B5 IRS1, L1448 mms, L1448 NW and L1527. Column densities and D/H ratios have been calculated, assuming optically thin transitions and an excitation temperature of 10 K, and are listed in Table 9. The upper limits on the [C_3HD]/[C_3H_2] ratios are consistent with observations made in L134N and TMC-1 (Bell et al. 1988), which found [C_3HD]/[C_3H_2] ∼ 0.1.

4. Discussion of results

Our values for [HDCO]/[H_2CO] and [DCN]/[HCN] are summarised in Fig. 3. The ratios for each source have been plotted against its bolometric temperature, which provides one way of measuring its evolutionary stage (Myers & Ladd 1993).

To determine the average fractionation, and test if fractionation is a function of evolutionary stage, we have calculated the least squares fits of a straight line to the data in Fig. 3. For the [HDCO]/[H_2CO] ratios a good fit could not be found to all the data points, however, when we left out the source HH211, which has a significantly lower HDCO fractionation, we obtained the fit shown as a solid line in Fig. 3a, with uncertainties on this fit shown as dashed lines. This suggests that, with the exception of HH211 and HH111, where [HDCO]/[H_2CO] ratios are 0.018 ± 0.003 and 0.029 ± 0.014, respectively, the observed [HDCO]/[H_2CO] ratios are all consistent with a value of 0.05–0.07.

Figure 3b shows the line of best fit to the observed [DCN]/[HCN] ratios (solid line), along with its associated uncertainty (dotted lines). With the exception of HH111, where [DCN]/[HCN] < 0.015, the best fit to our observed ratios is [DCN]/[HCN] ∼ 0.04, which remains flat as T_{bol} varies.

Figure 4a compares the linewidths of $H^{13}CN$ to DCN emission, and of $H_2^{13}CO$ to HDCO emission for each source, these being the lines we assumed to be optically thin. The linewidths are fairly similar, indicating that the emission from these molecules probably arose in the same region of the cloud, and so we are justified in taking ratios of the column densities. Figure 4b compares linewidths from H_2CO to HDCO and HCN to DCN in each source. HCN linewidths are fairly similar to DCN linewidths, however, the agreement between Δv for H_2CO and HDCO is not so good. This broadening is likely to be due to the optical depth in the H_2CO lines, since, for an opacity of 5, the line width is expected to increase by a factor of 1.7 (Phillips et al. 1979), which is close to the observed H_2CO vs. HDCO linewidth ratio for most sources.

Table 8. Column densities for HCN, $H^{13}CN$ and DCN and resulting [DCN]/[HCN] ratios.

Source	N(HCN) ($\times 10^{13}$ cm^{-2})	N($H^{13}CN$) ($\times 10^{12}$ cm^{-2})	N(DCN) ($\times 10^{12}$ cm^{-3})	$\frac{N(\mathrm{DCN})}{N(\mathrm{HCN})}$	$\frac{N(\mathrm{DCN})}{N(\mathrm{H^{13}CN})\times 60}$
B5 IRS1	2.85 (±0.37)	—	1.03 (±0.15)	0.036 (±0.007)	—
L1448 mms	8.54 (±0.68)	1.26 (±0.24)	3.52 (±0.39)	0.041 (±0.006)	0.047 (±0.010)
L1448 NW	6.77 (±0.40)	1.93 (±0.29)	4.35 (±0.44)	0.064 (±0.007)	0.038 (±0.007)
HH211	4.65 (±0.32)	0.85 (±0.15)	1.93 (±0.25)	0.042 (±0.006)	0.038 (±0.008)
IRAS 03282	3.32 (±0.30)	0.54 (±0.15)	1.37 (±0.16)	0.041 (±0.006)	0.042 (±0.013)
L1527	2.51 (±0.45)	0.40 (±0.10)	0.93 (±0.12)	0.037 (±0.008)	0.039 (±0.011)
L1551 IRS5	8.42 (±0.93)	0.51 (±0.10)	1.57 (±0.20)	0.019 (±0.003)	0.051 (±0.012)
RNO43	2.02 (±0.42)	<0.58	0.75 (±0.21)	0.037 (±0.013)	>0.022 (±0.006)
HH111	5.34 (±1.39)	<0.54	<0.82	<0.015	—

Table 9. Column densities of c-C_3HD and c-C_3H_2 and [C_3HD]/[C_3H_2] ratios.

Source	N(c-C_3H_2)[a] ($\times 10^{12}$cm^{-2})	N(c-C_3HD) ($\times 10^{12}$cm^{-2})	$\frac{[C_3HD]}{[C_3H_2]}$
B5 IRS1	—	0.77 (±0.33)	—
L1448 mms	>11.2	1.58 (±0.63)	<0.14 (±0.06)
L1448 NW	>9.9	1.59 (±0.69)	<0.16 (±0.07)
L1527	>8.4	2.30 (±0.31)	<0.27 (±0.04)

[a] From Buckle & Fuller (2001).

Table 10. The initial fractional abundances, relative to the total hydrogen density, used in our models.

Species	Abundance	Species	Abundance
H_2	5.00×10^{-1}	H_3^+	1.00×10^{-11}
He	1.40×10^{-1}	Si	2.00×10^{-8}
C^+	7.30×10^{-5}	Fe^+	1.00×10^{-8}
N	2.14×10^{-5}	S	1.00×10^{-7}
O	1.76×10^{-4}	HD	3.20×10^{-5}

5. The chemical models

Our observational results have been interpreted using detailed, chemical kinetic models of deuterium chemistry in dark clouds. The models, which are fully described in Roberts & Millar (2000a,b), now involve 298 species (135 of them containing deuterium) and ∼5550 reactions.

There are two basic models; the "gas-phase" model considers only reactions between gaseous species (with the exception that H_2 and HD can form on grain surfaces), while the "accretion" model includes the possibility that gas-phase species can collide with and stick to grains, essentially being removed from the gas.

In cold, dense gas, species which collide with dust grains are likely to stick; indeed, it is now well known that interstellar grains become encased in mantles of ice on a similar timescale to the dynamical and chemical evolution of molecular clouds (Willacy & Millar 1998; Rawlings 1999).

The deuterium fractionation, in particular, will be strongly affected. In cold clouds deuterium is extracted from its reservoir in HD by exothermic reactions such as

$$H_3^+ + HD \rightleftharpoons H_2D^+ + H_2 + \Delta E \quad (9)$$

which leads to an enhancement in the $[H_2D^+]/[H_3^+]$ ratio. Since both H_2D^+ and H_3^+ have extremely low proton affinities they rapidly react with species such as CO, C and H_2O, enhancing molecular D/H ratios throughout the system. In undepleted gas, reaction (9) represents a minor loss for H_3^+, however, as other species begin to freeze onto grain surfaces, reaction with HD becomes the dominant loss mechanism for H_3^+. As this produces H_2D^+, the $[H_2D^+]/[H_3^+]$ ratio increases further and results in an increase in all molecular D/H ratios for a time before most of the heavy species are removed from the gas.

This theoretical expectation, first predicted by Brown & Millar (1989), has recently been confirmed observationally by the detection of large $[DCO^+]/[HCO^+]$ ratios in L1544 in clumps in which CO is significantly depleted (Caselli et al. 1999). It may also prove important in explaining the large molecular D/H ratios observed towards IRAS 16293 and L134N.

All models presented in this paper use standard depleted solar elemental abundances for dark clouds, as listed in Table 10. We have adopted the cosmic D/H ratio measured by Linsky et al. (1995), 1.6×10^{-5}, a visual extinction of 10 mags and a cosmic ray ionisation rate of 1.3×10^{-17} s^{-1}.

5.1. A comparison with model results

Figure 5 shows the variation in [HDCO]/[H_2CO] and [DCN]/[HCN] with temperature and density, as predicted by our gas-phase models. Regardless of density, the model matches the observed [HDCO]/[H_2CO] ratios, 0.05–0.07, for a kinetic temperature between 10 and 20 K. However, the observed [DCN]/[HCN] ratios, of 0.04, are at least one and a half times larger than the model predicts, regardless of the physical conditions we assume, and ∼twice as large for reasonable density estimates (10^4–10^5 cm^{-3}).

It appears, therefore, that the gas-phase model alone is insufficient to explain the observations. There are, however, uncertainties inherent in any chemical modelling of this type. In particular, HCN, HNC and CN are all formed

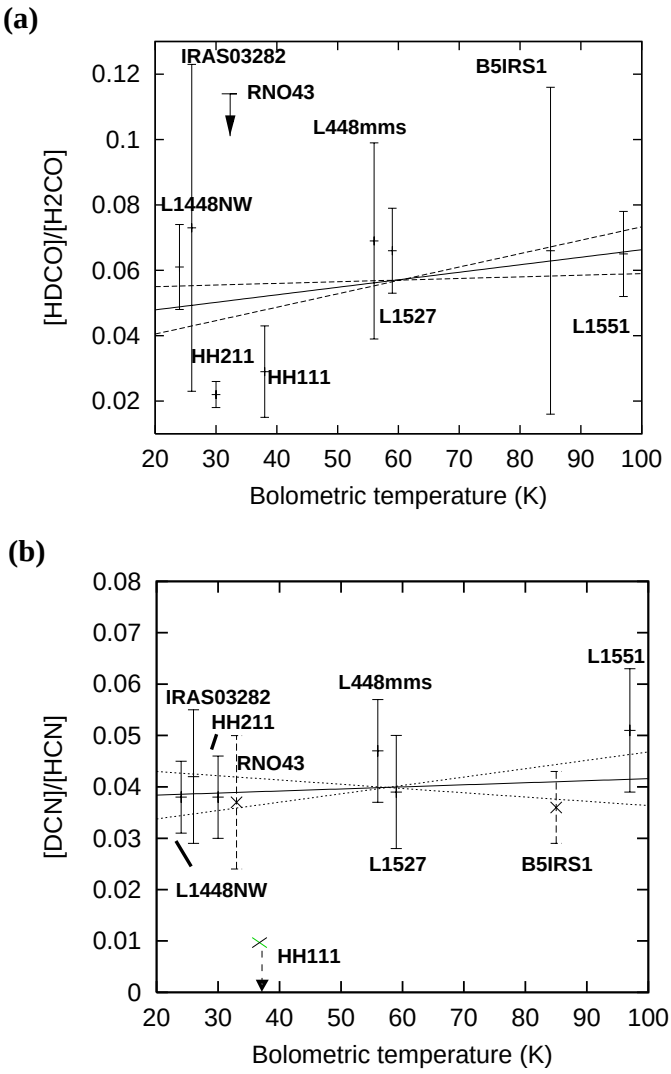

Fig. 3. A summary of our observed **a)** [HDCO]/[H_2CO] ratios (using $N(H_2^{12}CO)$) and **b)** [DCN]/[HCN] ratios (using $N(H^{13}CN)$ (solid error bars) and $N(H^{12}CN)$ (dashed error bars)), plotted against the bolometric temperature of the source, along with least-squares fits to the data (see text), arrows indicate upper limits.

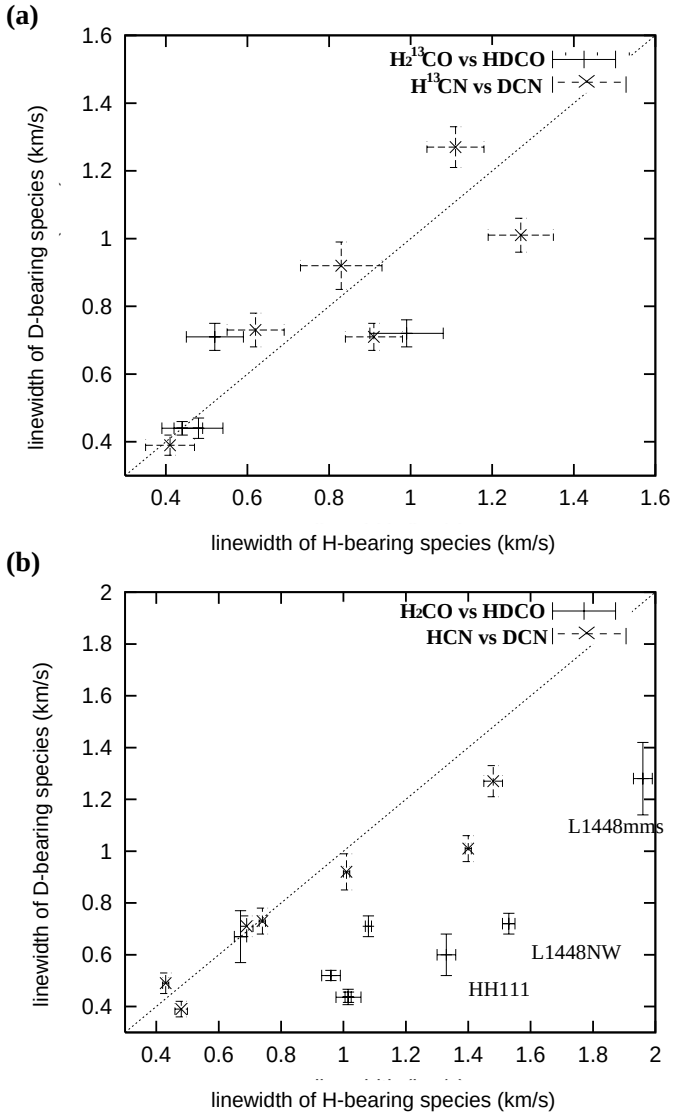

Fig. 4. A comparison of the linewidths of the molecules surveyed, the dotted line on each plot indicates equal widths; **a)** Δv for the ^{13}C-substituted isotopomers of H_2CO and HCN vs. Δv for the analogue deuterium-substituted molecules; **b)** Δv for the main isotopomers vs. Δv for the deuterium-substituted molecules.

via dissociative recombination of $HCNH^+$ with electrons, where our model assumes that 50% of the reactions form CN, while 25% form HCN and 25% form HNC (Herbst 1978). Recent experimental and observational work now suggests that HCN and HNC will be formed in equal amounts, but CN will not be formed by this reaction (Semaniak et al. 2001; Dickens et al. 2000). As there are analogue reactions for forming DCN and DNC, with same rate coefficients and branching ratios, this means that the abundances of HCN, HNC, DCN and DNC would all increase if we adopted these new branching ratios. However, we are primarily interested in abundance *ratios*, rather than absolute abundances, and as the deuterated and non-deuterated species are being affected in the same way, the molecular D/H ratios will be largely unchanged. We estimate that altering the branching ratios for recombination of $HCNH^+$ (and deuterated analogues) will not alter the predicted [DCN]/[HCN] ratio by more than 50%. It would still be too small to explain all the observations.

The accretion model, on the other hand, produces increased D/H ratios over the gas-phase model, as heavy species freeze out onto grain surfaces. Figure 6 compares results from the gas-phase and accretion models for [HDCO]/[H_2CO], [DCN]/[HCN] and other key molecular D/H ratios.

The [DCN]/[HCN] ratio is particularly sensitive to accretion, rising from its steady-state gas-phase value of 0.016 to match the observed ratios of 0.04 in $\sim 5 \times 10^4$ yrs. The DCN abundance is enhanced by constant cycling between DCN and $DCNH^+$, as $DCNH^+$ forms via proton transfer from H_3^+ and H_2D^+ to DCN, and via deuteron

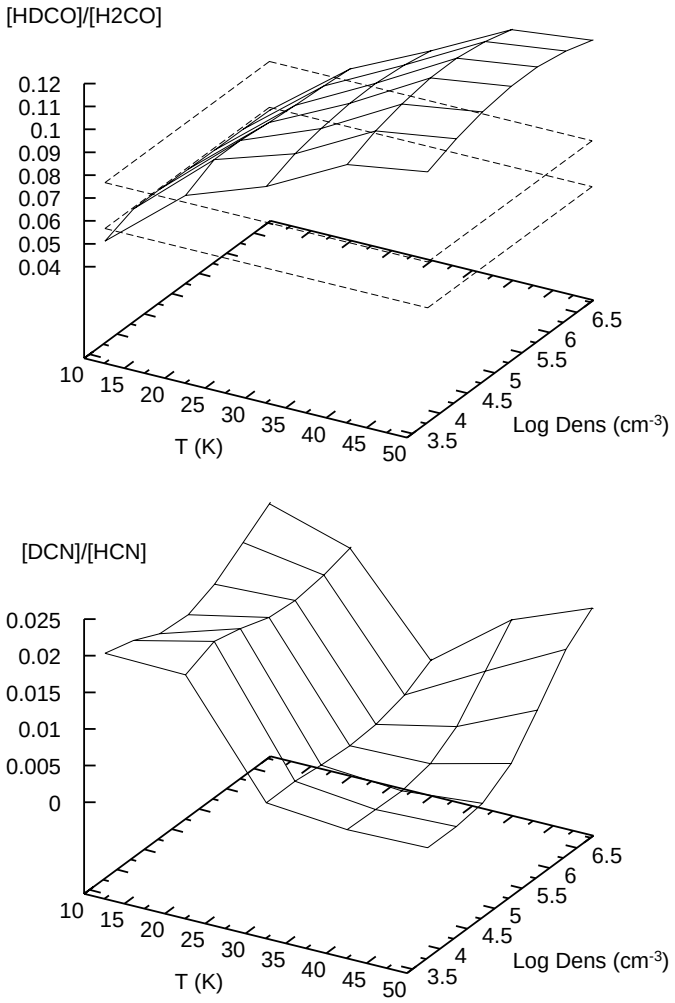

Fig. 5. Steady-state [HDCO]/[H$_2$CO] (top) and [DCN]/[HCN] (bottom) ratios, from our gas-phase models, varying over a temperature range 10–50 K (in intervals of 10 K) and a $\log_{10} n(\mathrm{H_2})$ range of ∼3.5–6.5 (in intervals of 0.5), the dashed planes indicate the observed [HDCO]/[H$_2$CO] ratios.

transfer from H_2D^+ to HNC. There are similar reactions which form HCN, and so, as the abundance of H_2D^+ increases, relative to H_3^+, there is an increased chance of forming DCN rather than HCN.

HDCO and H$_2$CO also react with H_2D^+ and H_3^+, forming the ions H_3CO^+ and H_2DCO^+ which may then recombine to H$_2$CO and HDCO, the increasing $[H_2D^+]/[H_3^+]$ ratio being reflected by the [HDCO]/[H$_2$CO] ratio. However, this is not the only route to forming H$_2$CO and HDCO, therefore, over the same time period the [HDCO]/[H$_2$CO] ratio, is not so sensitive to accretion processes. The ratio rises from 0.05 to 0.063, and so remains consistent with the ratios we measured towards the low-mass cores.

These results assume a kinetic temperature of 10 K and an H$_2$ density of 3×10^4 cm^{-3}. [DCN]/[HCN] ratios are sensitive to temperature (see Fig. 5), so if we assumed $T_{\rm kin} = 20$ K, the initial [DCN]/[HCN] ratio would be lower and it would take twice as long (10^5 yrs) for the predicted ratios to reach the levels we observed. As [HDCO]/[H$_2$CO] ratios increase with temperature for $T_{\rm kin} < 50$ K (see Fig. 5), predicted HDCO fractionation at this time would be much higher than was observed.

Changing the density in the accretion model primarily affects the timescale on which freeze-out occurs; increasing $n(\mathrm{H_2})$ from 3×10^4 to 10^5 cm^{-3} decreases the time it takes for the predicted [DCN]/[HCN] ratios to rise to agree with the observed values from 5×10^4 to $\sim 10^4$ yrs, and the time taken for everything to freeze out from $\sim 10^6$ to $\sim 3 \times 10^5$ yrs. On the other hand, if the density were lower, $\sim 10^4$ cm^{-3}, the predicted [DCN]/[HCN] ratio would not agree with the observed value until $\sim 2 \times 10^5$ yrs of accretion had occurred.

Table 11. Previous observations of formaldehyde and hydrogen cyanide towards a selection of interstellar sources.

Source	[H$_2$CO]	$\frac{[\mathrm{HDCO}]}{[\mathrm{H_2CO}]}$	[HCN]	$\frac{[\mathrm{DCN}]}{[\mathrm{HCN}]}$
IRAS 16293	2.0 $(-9)^1$	0.14^1	1.9 $(-9)^2$	0.01^2
L134N	2.0 $(-8)^3$	0.068^4	4.0 $(-9)^3$	0.05^4
TMC-1	7.0 $(-8)^5$	0.059^4	1.0 $(-8)^6$	0.011^4
OCR^a	3.7 $(-8)^7$	0.14^8	2.0 $(-8)^7$	0.04^9
OHC^b	2.6 $(-8)^7$	—	3.0 $(-7)^7$	0.003^9

NOTES: $a(-b)$ implies $a \times 10^{-b}$.
^{a} Orion Compact Ridge; ^{b} Orion Hot Core.
REFS: 1. Loinard et al. (2000); 2. van Dishoeck et al. (1995); 3. Ohishi et al. (1992); 4. Turner (2001); 5. Ohishi (1998); 6. Willacy & Millar (1998); 7. Charnley et al. (1992); 8. Turner (1990); 9. Schilke et al. (1992).

6. A comparison with previous observations

Table 11 lists the [HDCO]/[H$_2$CO] and [DCN]/[HCN] ratios which have been observed towards other sources. A major motivation for this study was to see if the high [HDCO]/[H$_2$CO] ratios and low [DCN]/[HCN] ratios seen towards IRAS 16293 are typical of low-mass star formation. Instead, we found [HDCO]/[H$_2$CO] ratios less than half of the value observed towards IRAS 16293 and the Orion Compact Ridge (OCR), and slightly lower than those seen in the cold cloud TMC-1. [DCN]/[HCN] ratios, on the other hand, appear to be significantly higher than are seen towards both TMC-1 and IRAS 16293, but similar to those seen towards the OCR. The [DCN]/[HCN] ratios we have observed are also similar to those measured in L134N (Turner 2001), a source where $[DCO^+]/[HCO^+]$, $[NH_2D]/[NH_3]$ and $[NHD_2]/[NH_3]$ ratios are also enhanced over cold cloud values (Tiné et al. 2000; Roueff et al. 2000).

6.1. Low-mass star-forming cores

Shah & Wootten (2001) have observed $[NH_2D]/[NH_3]$ and $[DCO^+]/[HCO^+]$ ratios towards a wide range of low-mass, protostellar cores. Their source list overlaps, to some extent, with ours, the relevant results being included in Table 12. The $[NH_2D]/[NH_3]$ ratio towards IRAS 03282 is 0.007, slightly lower than that predicted by the gas-phase chemical model at steady state (∼0.015 at 10 K),

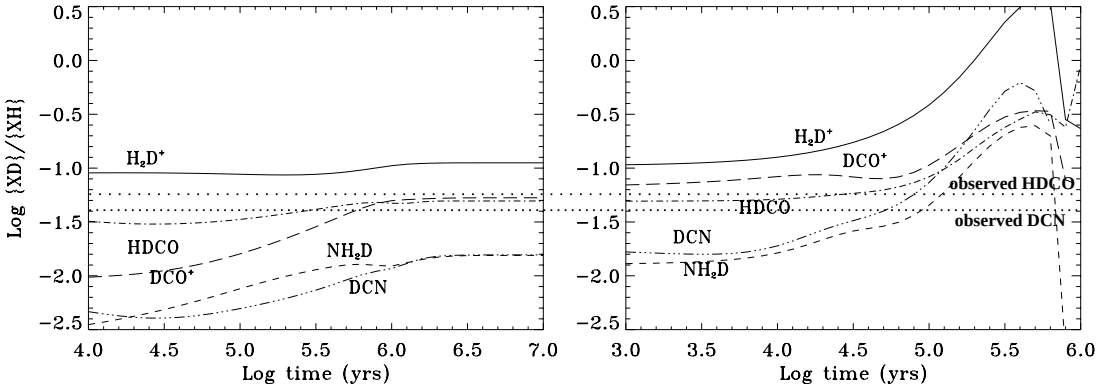

Fig. 6. Molecular D/H ratios evolving over time from our gas-phase (left) and accretion (right) models; $T_{\rm kin} = 10$ K, $n(H_2) = 3 \times 10^4$ cm^{-3}. The best fits to the [HDCO]/[H_2CO] and [DCN]/[HCN] ratios we observed are also indicated on the plots.

Table 12. Observations of other molecular D/H ratios towards the sources in our survey (for the data from Butner et al. (1995), ratios have been recalculated for a $^{12}C/^{13}C$ ratio of 60).

Source	[DCO^+]/[HCO^+]	[NH_2D]/[NH_3]
B5 IRS1	0.039[1]	
L1448 mms	0.013 ($\pm$0.004)[2]	0.029 ($\pm$0.011)[2]
L1448 NW		0.09 ($\pm$0.02)[2]
IRAS 03282		0.007 ($\pm$0.003)[2]
L1527	0.019 ($\pm$0.005)[2]	
L1551 IRS5	0.035[3]/0.084[1]	0.087 ($\pm$0.013)[2]

REFS: 1. Butner et al. (1995); 2. Shah & Wootten (2001); 3. Williams et al. (1998).

however higher ratios were seen towards other sources. [NH_2D]/[NH_3] ratios are also expected to rise as accretion occurs, see Fig. 6, and after 5×10^4 yrs the predicted ratio has risen to 0.03, the value observed towards L1448 mms, but it takes almost 2×10^5 yrs of accretion to increase the [NH_2D]/[NH_3] ratio to $\sim$0.09, as was observed towards L1551 IRS5 and L1448 NW.

DCO^+ is fractionated directly via deuteron transfer from H_2D^+, therefore [DCO^+]/[HCO^+] ratios are expected to be among the highest molecular D/H ratios. This is illustrated in Fig. 6, the steady-state [DCO^+]/[HCO^+] ratio from the gas-phase model, 0.05, rising to $\sim$0.08 after 5×10^4 yrs of accretion. The [DCO^+]/[HCO^+] ratio observed towards L1551 IRS5 by Butner et al. (1995) is similar to this value, but most of the [DCO^+]/[HCO^+] ratios observed by Shah & Wootten towards the sources in our survey are lower even than the gas-phase models predict (see Table 12). However, more detailed observations (Shah 2000), indicate that the DCO^+ emission may be arising from a different region to the HCO^+, thus, these [DCO^+]/[HCO^+] ratios are very sensitive to the precise details of the radiative transfer model used. Alternatively, this relatively low DCO^+ fractionation may simply be evidence that accretion is not currently occurring in these sources, but occurred during an earlier stage of evolution.

Another source which has been observed to have high [DCN]/[HCN] and [NH_2D]/[NH_3] ratios (0.04 and 0.06, respectively), but relatively low DCO^+ fractionation (0.002) is the Orion Compact Ridge (OCR).

Despite the fact that both are classed as hot cores, there are marked chemical differences between the OCR and the Orion Hot Core (OHC) which have been noted by previous workers. It appears that both contain species which have been evaporated from grain surfaces, however, the ice mantles in the OHC seem to have been ammonia rich and methanol poor, while the OCR mantles were methanol rich but ammonia poor.

Levels of deuterium fractionation also differ between the OHC and the OCR. Most ratios which have been measured towards the OHC are $\sim 10^{-3}$, similar to other hot cores. However, several of the deuterated species observed towards the OCR, including HDCO and DCN, have levels of fractionation similar to or even larger than is seen towards the cold cloud TMC-1.

If the Hot Core formed earlier in the evolution of the ridge cloud, when the gas was mostly atomic, surface hydrogenation would produce species such as NH_3, CH_4 and H_2O, with deuterium fractionation which reflects the atomic D/H ratio in the accreting gas (Charnley et al. 1992; Hatchell et al. 1999). In the Compact Ridge, forming at a later time when the accreting gas was mostly molecular, accretion over a longer timescale at low temperatures may have increased deuterium fractionation. CO in the gas-phase would then form H_2CO and CH_3OH on the grain surfaces, and deuterium fractionation would be higher in most species.

On the other hand, the differences between the OHC and the OCR could be due to their forming at different temperatures and/or densities (Caselli et al. 1992). Higher temperatures during the collapse phase of the Hot Core would supress deuterium fractionation, and could also mean that CO did not stay on the grain surfaces long enough for significant amounts of H_2CO and CH_3OH to form.

6.2. A comparison with high-mass star formation

Hatchell et al. (1998) conducted a survey of [DCN]/[HCN] ratios towards several HMC's, finding ratios typically (0.9–4.1) $\times 10^{-3}$, later searches for HDS (Hatchell et al. 1999) put limits on [HDS]/[H_2S] ratios of $\leq 10^{-3}$. These values are very similar, and point either to grain surface processing acting to reduce molecular D/H ratios from cold cloud values, or, as deuterium fractionation is so sensitive to temperature variations, to higher temperatures ($\geq$30 K) at the time the molecules froze onto the grain surfaces.

This appears to contrast with levels of deuterium fractionation observed towards low-mass star forming cores. van Dishoeck et al. (1995) measured [HDS]/[H_2S] $\sim$ 0.1 towards IRAS 16293, we have measured [DCN]/[HCN] $\sim$ 0.04 towards other low-mass cores. Both these ratios are higher than those observed towards HMC's or predicted by chemical models.

To form stars, cold, dense clouds, with enhanced D/H ratios, collapse under gravity. Gas phase molecules then freeze onto grain surfaces, possibly undergoing some chemical processing, before a shock or outflow disrupts the grains and evaporates their mantles. The fact that this sequence of events produces such different levels of deuterium fractionation in HMC's and low-mass cores may, as in the case of the OHC and the OCR, point to significant evolutionary differences between these two types of star forming region.

Higher temperatures during the pre-collapse phase of high mass stars has already been suggested as an explanation for the lower molecular D/H ratios in HMC's and for the chemical differences between the Orion Hot Core and Compact Ridge. It might also be the case that the longer collapse timescales associated with low-mass star formation mean that accretion processes have significantly impacted on the chemistry in these regions.

7. Discussion

We have measured [HDCO]/[H_2CO] and [DCN]/[HCN] ratios towards a selection of Class 0 and Class I low-mass, protostellar cores, towards three different star forming regions.

Least-squares fits to our data gave [HDCO]/[H_2CO] $\sim$ 0.05–0.07, consistent with predictions from a gas-phase model at 10 K. Most [DCN]/[HCN] ratios were $\sim$0.04, higher than gas-phase models predict, but similar to ratios observed towards L134N and the Orion Compact Ridge.

There are no significant differences between the three different star forming regions we surveyed, or betwen Class 0 and Class I sources. This implies that deuterium fractionation is not being affected by shocks, mantle evaporation or accretion after the Class 0 stage, but is set earlier in the history of the collapsing cloud.

We have used detailed chemical, kinetic models of deuterium fractionation in order to match our observed [HDCO]/[H_2CO] and [DCN]/[HCN] ratios. We find best agreement between model predictions and observations by assuming that accretion of molecules onto grains has impacted on the chemistry over a time period of about 50 000 years. This is a measure of the timescale over which the gas was cold and dense before forming a protostar. Although it does depend on the density of the gas, the shortness of this period argues that the evolution to high density and the collapse to form a protostar with an outflow occur very rapidly.

The similarity between the [DCN]/[HCN] ratios observed towards these low-mass protostellar cores and those seen in L134N, along with their marked difference from [DCN]/[HCN] ratios observed in high-mass star forming regions, leads us to suggest that there are significant chemical differences between high and low mass star forming regions.

For both high and low mass star forming regions, qualitatively similar processes are occurring. Cold, dense cores, with enhanced deuterium fractionation, begin to contract under gravity. Gas phase species collide with and stick to dust grains, building up mantles of ice in which the species can be oxidised or reduced. Once these cores form a protostar, which heats or disrupts (via an outflow) its surrounding envelope, the grain mantles are released back into the gas-phase. The chemical composition in these cores after evaporation will, therefore, depend on the composition of the ice mantles.

Recent observations (e.g. van der Tak et al. 2000; Nummelin et al. 2001) suggest that ice composition may varies between different environments. These differences may be due to the precise details of the surface chemistry which is occurring (as yet, not well understood), or they may depend on the degree of processing (e.g. by u.v. radiation or cosmic rays) that the ice undergoes. However, the deuterium fractionation within these ices, is likely to be most sensitive to the temperatures and densities under which they formed.

High mass stars appear to form at higher temperatures and densities so molecular D/H ratios which evaporate from grain surfaces in the hot cores close by are lower than those seen in cold clouds. Low mass stars, on the other hand, form at lower temperatures and over longer timescales which means that accretion can impact on the chemistry leading to levels of deuterium fractionation similar to or higher than in dark clouds.

Acknowledgements. HR is grateful to PPARC for the award of a studentship. Astrophysics at UMIST is supported by PPARC. The 12 m Telescope is a facility of the National Science Foundation currently operated by the University of Arizona Steward Observatory under a loan agreement with the National Radio Astronomy Observatory.

References

Bell, M. B., Avery, L. W., Matthews, H. E., et al. 1988, ApJ, 326, 924

Brown, P. D., & Millar, T. J. 1989, MNRAS, 237, 661

Buckle, J. V. 2001, Ph.D. Thesis, UMIST
Buckle, J. V., & Fuller, G. A. 2001, A&A, submitted
Butner, H. M., Lada, E. A., & Loren, R. B. 1995 ApJ, 448, 207
Caselli, P., Hasegawa, T. I., & Herbst, E. 1993, ApJ, 408, 548
Caselli, P., Walmsley, C. M., Tafalla, M., Dore, L., & Myers, P. C. 1999, ApJ, 523, L165
Charnley, S. B., Tielens, A. G. G. M., & Millar, T. J. 1992, ApJ, 399, L71
Dickens, J. E., & Irvine, W. M. 1999, ApJ, 518, 733
Dickens, J. E., Irvine, W. M., Snell, R. L., et al. 2000, ApJ, 542, 870
Goldsmith, P. F., & Langer, W. D. 1999, ApJ, 517, 209
Hatchell, J., Millar, T. J., & Rodgers, S. D. 1998, A&A, 332, 695
Hatchell, J., Roberts, H., & Millar, T. J. 1999, A&A, 346, 227
Herbst, E. 1978, ApJ, 222, 508
Kahane, C., Frerking, M. A., Langer, W. D., Encrenaz, P., & Lucas, R. 1984, A&A, 137, 211
Ladd, E. F., Fuller, G. A., & Deane, J. R. 1998, ApJ, 495, 871
Linsky, J. L., Diplas, A., Wood, B. E., et al. 1995, ApJ, 451, 335
Loinard, L., Castets, A., Ceccareli, C., et al. 2000, A&A, 359, 1169
Minh, Y. C., Dickens, J. E., Irvine, W. M., & McGonagle, D. 1995, A&A, 298, 213
Myers, P. C., & Ladd, E. F. 1993, ApJ, 413, L47
Nummelin, A., Whittet, D. C. B., Gibb, E. L., Gerakines, P. A., & Chiar, J. E. 2001, ApJ, 558, 185
Ohishi, M., Irvine, W. M., & Kaifu, N. 1992, in The Astrochemistry of Cosmic Phenomena, ed. P. D. Singh (Dordecht: Kluwer), IAU Symp., 150, 171
Ohishi, M., & Kaifu, N. 1998, Faraday Dis., 109, 205
Phillips, T. G., Huggins, P. J., Wannier, P. G., & Scoville, N. Z. 1979, ApJ, 231, 720
Rawlings, J. M. C. 2000, in Astrochemistry: From molecular clouds to planetary systems, ed. Y. C. Monh, & E. F. van Dishoeck (San Francisco ASP), IAU Symp. 197, 15
Roberts, H., & Millar T. J. 2000a, A&A, 361, 388
Roberts, H., & Millar, T. J. 2000b, A&A, 364, 780
Rodgers, S. D., & Millar, T. J. 1996, MNRAS, 280, 1046
Roueff, E., Tiné, S., Coudert, L. H., et al. 2000, A&A, 354, L63
Semaniak, J., Minaev, B. F., Derkatch, A. M., et al. 2001, ApJS, 135, 275
Schilke, P., Walmsley, C. M., Pineau des Forêts, G., et al. 1992, A&A, 256, 595
Shah, R. Y. 2000, Ph.D. Thesis, University of Virginia
Shah, R. Y., & Wootten, A. 2001, ApJ, 554, 933
Stutzki, J., Genzel, R., Graf, U. U., & Harris, A. I. 1989, ApJ, 340, L37
Tiné, S., Roueff, E., Falgarone, E., Gerin, M., & Pineau des Forêts, G. 2000, A&A, 356, 1039
Turner, B. E. 1990, ApJ, 362, L29
Turner, B. E. 2001, ApJS, in press
van der Tak, F. F. S., van Dishoeck, E. F., & Caselli, P. 2000, A&A, 361, 327
van Dishoeck, E. F., Blake, G. A., Jansen, D. J., & Groesbeck, T. D. 1995, ApJ, 447, 760
Willacy, K., & Millar, T. J. 1998, MNRAS, 298, 562
Williams, J. P., Bergin, E. A., Caselli, P., Myers, P. C., & Plume, R. 1998, ApJ, 503, 689
Wright, M. C. H., Plambeck, R. L., & Wilner, D. J. 1996, ApJ, 469, 216
Wyrowski, F., Schilke, P., & Walmsley, C. M. 1999, A&A, 341, 882